Molecular Cell
Article

Staufen1-Mediated mRNA Decay Functions in Adipogenesis

Hana Cho,[1] Kyoung Mi Kim,[1] Sisu Han,[1] Junho Choe,[1] Seung Gu Park,[2] Sun Shim Choi,[2] and Yoon Ki Kim[1,*]
[1]School of Life Sciences and Biotechnology, Korea University, Seoul 136-701, Republic of Korea
[2]Department of Medical Biotechnology, College of Biomedical Science, and Institute of Bioscience and Biotechnology, Kangwon National University, Chuncheon 200-701, Republic of Korea
*Correspondence: yk-kim@korea.ac.kr
DOI 10.1016/j.molcel.2012.03.009

SUMMARY

The double-stranded RNA binding protein Staufen1 (Stau1) is involved in diverse gene expression pathways. For Stau1-mediated mRNA decay (SMD) in mammals, Stau1 binds to the 3′ untranslated region of target mRNA and recruits Upf1 to elicit rapid mRNA degradation. However, the events downstream of Upf1 recruitment and the biological importance of SMD remain unclear. Here we show that SMD involves PNRC2, decapping activity, and 5′-to-3′ exonucleolytic activity. In particular, Upf1 serves as an adaptor protein for the association of PNRC2 and Stau1. During adipogenesis, Stau1 and PNRC2 increase in abundance, Upf1 becomes hyperphosphorylated, and consequently SMD efficiency is enhanced. Intriguingly, downregulation of SMD components attenuates adipogenesis in a way that is rescued by downregulation of an antiadipogenic factor, Krüppel-like factor 2 (KLF2), the mRNA of which is identified as a substrate of SMD. Our data thus identify a biological role for SMD in adipogenesis.

INTRODUCTION

The double-stranded RNA-binding protein Staufen (Stau) plays multiple roles in gene expression. *Drosophila* Stau is involved in the localization of maternal mRNAs in oocyte and egg (Roegiers and Jan, 2000). Similarly, mammalian Stau also participates in mRNA localization in vertebrate neurons and oocytes (Maquat and Gong, 2009; Miki et al., 2005). Mammalian cells contain two paralogues of Stau, Staufen1 (Stau1) and Staufen2 (Stau2), both of which associate with a broad spectrum of mRNAs (Maquat and Gong, 2009; Miki et al., 2005). In addition to its role in mRNA localization, when Stau1 binds to a Stau1-binding site (SBS) in the 3′ untranslated region (3′UTR) of target mRNAs, Stau1 can induce mRNA degradation called Stau1-mediated mRNA decay (SMD) (Gong et al., 2009; Gong and Maquat, 2011; Kim et al., 2005, 2007).

Efficient SMD requires a translation termination event, Stau1, and Upf1 (Kim et al., 2005). When translation terminates sufficiently upstream of a SBS, the SBS-bound Stau1 recruits Upf1, probably via protein-protein interaction, so as to induce mRNA degradation (Kim et al., 2005). SBS can be formed either by intramolecular base pairing in the 3′UTR of the target mRNA or by intermolecular base pairing between an Alu sequence in the 3′UTR of the target mRNA and another Alu sequence in a long noncoding RNA (lncRNA) (Gong and Maquat, 2011). SMD may influence a wide spectrum of physiological events by targeting several types of cellular substrates (Gong et al., 2009; Kim et al., 2005, 2007).

A translation termination event and Upf1 are also required for a related mRNA decay mechanism: nonsense-mediated mRNA decay (NMD) (Durand and Lykke-Andersen, 2011; Neu-Yilik and Kulozik, 2008; Nicholson et al., 2010; Rebbapragada and Lykke-Andersen, 2009). NMD recognizes aberrant transcripts harboring a premature termination codon (PTC) and downregulates the abundance of those mRNAs. In addition, NMD is considered one of the posttranscriptional regulation mechanisms that target cellular transcripts (Mendell et al., 2004). The terminating ribosome on a PTC recruits a so-called SURF complex that consists of SMG1 kinase, Upf1, and eukaryotic translation release factors (eRFs) 1 and 3. Upf1 in the SURF complex binds to a PTC-distal exon junction complex (EJC), which is deposited 20–24 nucleotides upstream of most exon-exon junctions as a result of splicing. An interaction between Upf1 and a PTC-distal EJC triggers Upf1 phosphorylation by SMG1 kinase (Kashima et al., 2006; Yamashita et al., 2005, 2009). Phosphorylated Upf1 recruits SMG5, SMG6, SMG7, or proline-rich nuclear receptor coregulatory protein 2 (PNRC2), consequently triggering the decay of PTC-containing mRNA in an exonucleolytic and/or endonucleolytic manner (Cho et al., 2009; Eberle et al., 2009; Fukuhara et al., 2005; Huntzinger et al., 2008; Unterholzner and Izaurralde, 2004). It has been shown that PNRC2 links the terminating ribosome on the PTC and the decapping complex and triggers movement of the PTC-containing mRNP to processing bodies (P bodies) (Cho et al., 2009), where mRNAs destined for degradation are stored or degraded (Eulalio et al., 2007; Parker and Sheth, 2007). In contrast to NMD, it is not yet clear how Upf1 recruited by Stau1 triggers the decay of SMD substrates.

Adipogenesis is a cell differentiation process by which preadipocytes differentiate into adipocytes. Adipose tissue plays an essential role in many biological processes including hemostasis, the immune response, blood pressure control, energy balance, and glucose homeostasis (Rosen and MacDougald,

2006). Adipogenesis is coordinated by a complex network of transcriptional cascades (Darlington et al., 1998; Rosen and MacDougald, 2006; Rosen and Spiegelman, 2000). Peroxisome proliferator-activated receptor γ (PPARγ) is a key transcription factor in adipogenesis. When activated, PPARγ induces almost all of the genes that are characteristic of fat cells, along with morphological changes of cells and lipid accumulation. Several positive and negative regulators control the expression of PPARγ. Two CCAAT/enhancer-binding proteins (C/EBPs), C/EBP-β and C/EBP-δ, induce PPAR-γ expression in the early stage of adipogenesis. On the other hand, C/EBPα is involved in the maintenance of PPARγ expression (Darlington et al., 1998). Krüppel-like factors (KLFs) have also been implicated in adipogenesis. KLF5 and KLF15 function as positive regulators, while KLF2 functions as a negative regulator (Rosen and MacDougald, 2006; Rosen and Spiegelman, 2000).

In this study, we provide several lines of evidence demonstrating that, in SMD, the downstream steps after Upf1 recruitment involve PNRC2. More importantly, our observations in 3T3-L1 cells indicate an essential role for SMD in adipogenesis.

RESULTS

SMD Requires PNRC2, Decapping Activity, and 5′-to-3′ Exonucleolytic Activity

Recently, our group identified PNRC2 as a Upf1- and Dcp1a-interacting protein, and we proposed that PNRC2 links the mRNA surveillance machinery and the decapping complex, triggering 5′-to-3′ decay of NMD substrates (Cho et al., 2009). To investigate how many cellular NMD substrates require PNRC2 for decay, we carried out microarray analysis using HeLa cells depleted of either endogenous Upf1 or PNRC2 through specific siRNA (Figure 1A).

Microarray analyses using 24K human gene chips revealed that 761 and 648 transcripts were upregulated by at least 1.5-fold upon Upf1 and PNRC2 downregulation, respectively. Among them, 201 transcripts (out of 648 transcripts, ~31%) were commonly upregulated (see Table S1 available online). Notably, 50% of the commonly upregulated transcripts (100 out of 201) contained the known NMD-inducing features (Mendell et al., 2004): upstream open reading frames (uORFs) in the 5′UTR, introns in the 3′UTR, alternative splicing variants that harbor nonsense codons, and selenocysteine codons (Figure 1B). The simple interpretation of these results is that at least 30% of endogenous NMD substrates require PNRC2 for decay.

Intriguingly, we also observed that serine (or cysteine) proteinase inhibitor clade E (nexin plasminogen activator inhibitor type 1) member 1 (SERPINE1) mRNA and v-jun sarcoma virus 17 oncogene homolog (avian) (c-JUN) mRNA, both of which are SMD substrates (Kim et al., 2005; Kim et al., 2007), were among the commonly upregulated transcripts (Table S1). These observations led us to hypothesize that PNRC2 is involved in SMD. To test this hypothesis, we first confirmed the microarray results using quantitative real-time RT-PCR (qRT-PCR) with total RNAs purified from HeLa cells depleted of endogenous Stau1, PNRC2, Upf1, or Upf2 (Figures 1C and 1D and Table S1A). Previous studies showed that whereas SMD involves Stau1 and Upf1, NMD involves PNRC2, Upf1, and Upf2 (Cho et al., 2009; Gong et al., 2009; Kim et al., 2005, 2007). Western blotting results demonstrated that siRNA transfection specifically reduced the levels of endogenous Stau1, PNRC2, Upf1, and Upf2 to 5%, 29%, 9%, and 14%, respectively, of normal levels (Figure 1C). qRT-PCR revealed that downregulation of Stau1, PNRC2, and Upf1 inhibited SMD of endogenous SERPINE1 mRNA by 2.4-, 2.8-, and 3.9-fold, respectively (Figure 1D), and of endogenous c-JUN mRNA by 2.6-, 5.2-, and 2.4-fold, respectively (Figure S1A). As expected, downregulation of Upf2 had no significant effect on the levels of either mRNA. These results suggest that SMD involves PNRC2.

Based on our previous report of an interaction between PNRC2 and Dcp1a (Cho et al., 2009), we further tested whether SMD involves decapping activity and 5′-to-3′ exonucleolytic activity. To this end, cells were depleted of endogenous Dcp2, which is a decapping enzyme complexed with Dcp1a, or Xrn1, which is a 5′-to-3′ exoribonuclease (Figures 1E and 1F and Figure S1B). Western blotting results showed that the levels of endogenous Stau1, Dcp2, and Xrn1 were specifically reduced to 9%, 30%, and 3% of normal, respectively (Figure 1E). Both SERPINE1 mRNA (Figure 1F) and c-JUN mRNA (Figure S1B) increased by ~2-fold upon downregulation of Dcp2 or Xrn1. More importantly, the half-life of SERPINE1 mRNA was significantly increased upon downregulation of Stau1, PNRC2, Upf1, Dcp2, or Xrn1, but not Upf2 (Figure 1G). All together, our findings suggest that SMD involves PNRC2, decapping activity, and 5′-to-3′ exonucleolytic activity.

Stau1 Is Complexed with Upf1, PNRC2, and Dcp1a

Our findings that SMD involves PNRC2 (Figure 1) led us to test whether PNRC2, Upf1, and Stau1 associate with each other. To this end, HEK293T cells were transiently cotransfected with plasmids expressing Myc-PNRC2, FLAG-Upf1, and Stau1^{55}-HA$_3$ (Figure 2A and Figures S2B and S2C). Western blotting results showed that the abundance of FLAG-Upf1, Myc-PNRC2, and Stau1^{55}-HA$_3$ was equal to or less than that of endogenous protein (Figure S2A). The results of immunoprecipitation (IP) revealed that Myc-PNRC2 and Stau1^{55}-HA$_3$ coimmunopurified with FLAG-Upf1 in a partially RNase-resistant manner (Figure 2A, upper), consistent with our previous report (Cho et al., 2009). Efficient removal of RNAs by RNase A treatment was demonstrated by RT-PCR of endogenous GAPDH mRNAs using α-[^{32}P]-dATP and specific oligonucleotides (Figure 2A, lower). The reciprocal IPs also demonstrated the specific associations among these proteins (Figures S2B and S2C). Furthermore, Stau1^{55}-HA$_3$ coimmunopurified with FLAG-Dcp1a (Figure S2D). More importantly, we also observed that endogenous Stau1 and PNRC2 coimmunopurified with endogenous Upf1 (Figure 5C). All these results suggest that Stau1 is complexed with Upf1, PNRC2, and Dcp1a.

Upf1 Serves as an Adaptor Protein for the Association of PNRC2 and Stau1

Considering that (1) PNRC2 interacts with the C-terminal two-thirds of Upf1 spanning amino acids 419–1,118 (Figures S2E and S2F) and (2) Stau1 associates with the N terminus (amino acids 1–244) of Upf1 (Gong et al., 2009), Upf1 may function to

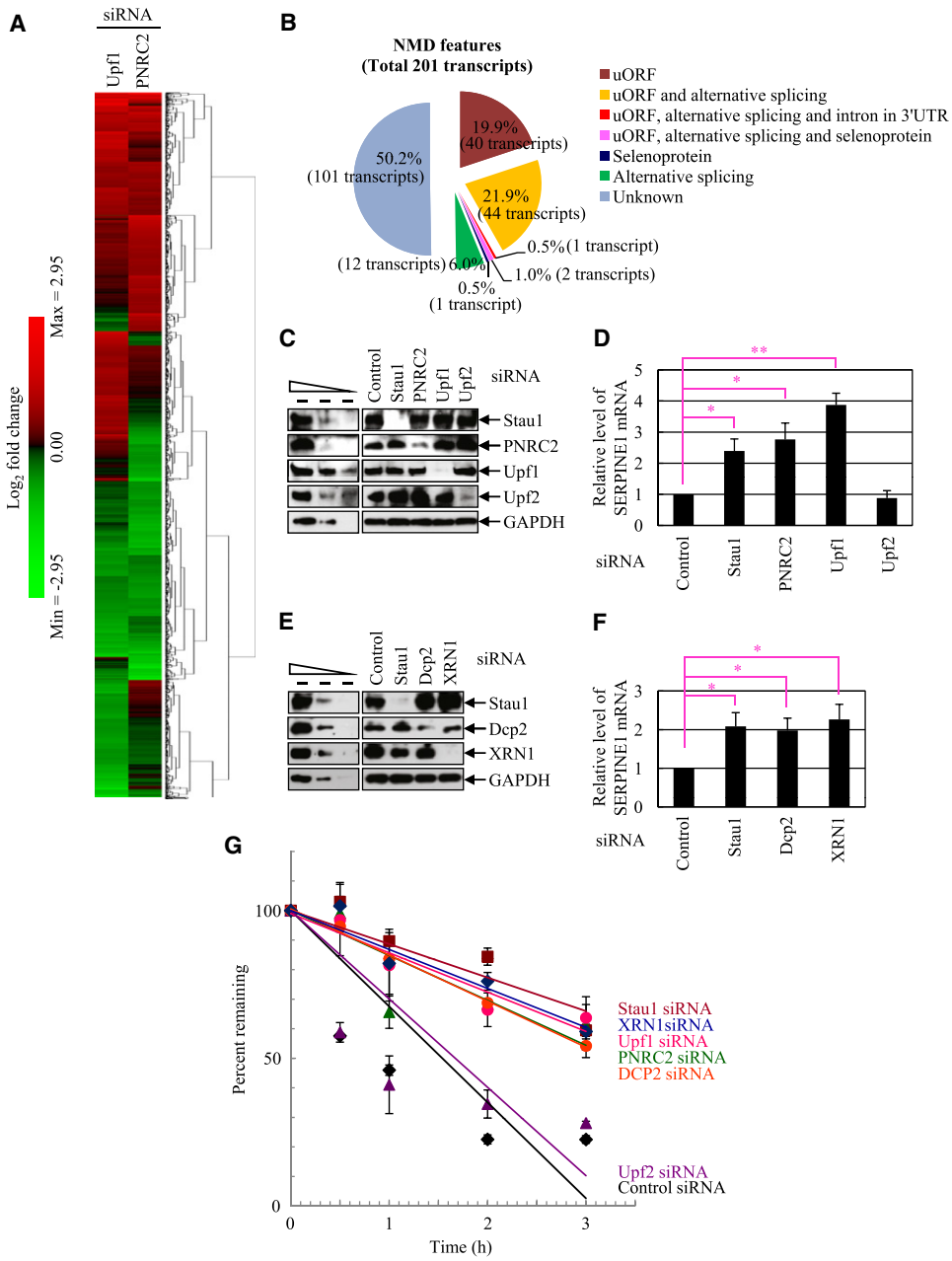

Figure 1. SMD Involves PNRC2, Upf1, Stau1, Decapping Activity, and 5′-to-3′ Exoribonucleolytic Activity

(A) Cluster analysis of normalized microarray expression data from HeLa cells depleted of either Upf1 or PNRC2.

(B) NMD-inducing features in the commonly upregulated transcripts.

(C–F) HeLa cells were transiently transfected with the indicated siRNAs. Three days later, total-cell proteins and RNAs were prepared and analyzed by western blotting and quantitative real-time RT-PCR (qRT-PCR), respectively. (C and E) Western blotting to demonstrate specific downregulation by siRNAs. Cellular GAPDH served as a control for variations in protein loading. To demonstrate that the western blotting was semiquantitative, 3-fold serial dilutions of total-cell extracts were loaded in the three leftmost lanes. (D and F) qRT-PCRs of endogenous SERPINE1 mRNA. The level of endogenous SERPINE1 mRNA was normalized to the level of endogenous SMG7 mRNA. Normalized level in the presence of Control siRNA was set to 1.0.

(G) Half-life of endogenous SERPINE1 mRNAs. HeLa cells were transiently transfected with the indicated siRNAs. Three days later, cells were treated with 100 μg/ml 5,6-dichloro-1-β-D-ribofuranosylbenzimidazole (DRB) to block transcription. Total-cell RNAs were purified at the indicated time points and analyzed by qRT-PCR. The levels of endogenous SERPINE1 mRNAs, which were normalized to GAPDH mRNA, were plotted as a function of time after DRB treatment.

The columns and error bars in (D), (F), and (G) represent the mean and standard deviation of at least two independently performed transfections and qRT-PCRs. Two-tailed, equal-sample variance Student's t tests were used to calculate the P values (**$p < 0.01$; *$p < 0.05$). See also Figure S1 and Table S1.

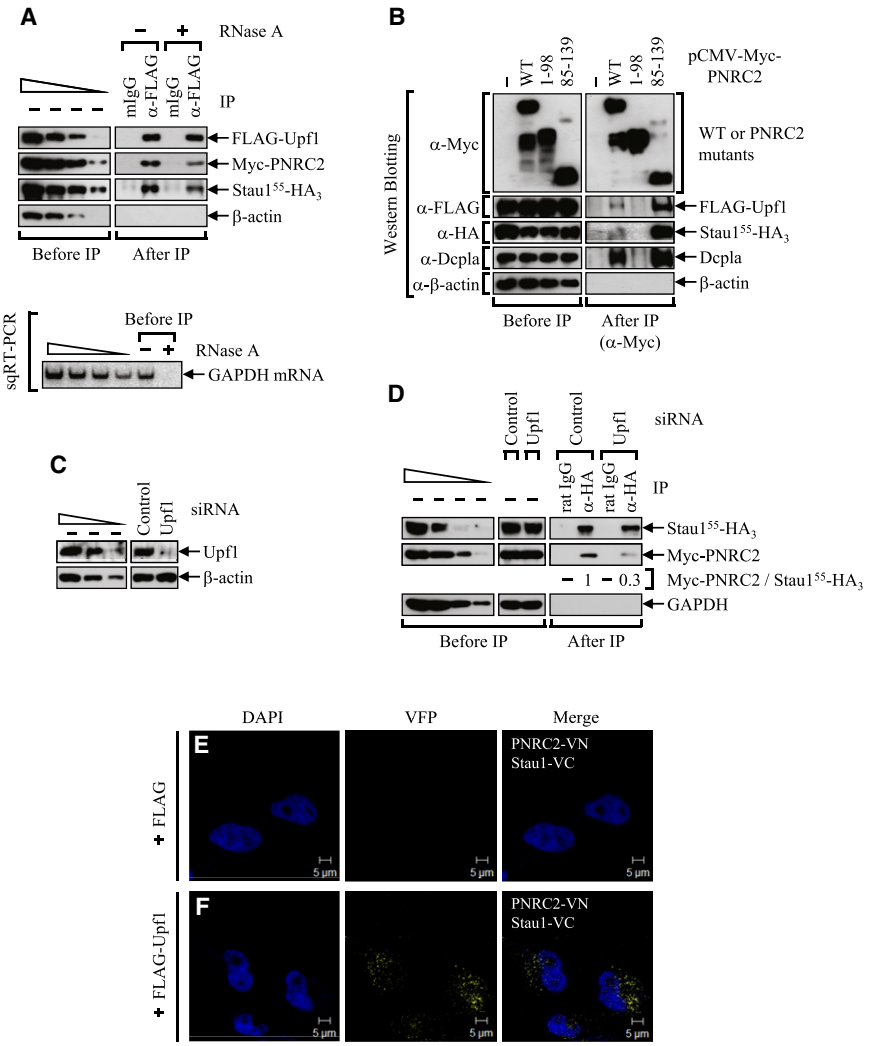

Figure 2. Stau1 Is Complexed with Upf1, Dcp1a, and PNRC2, and Upf1 Serves as an Adaptor Protein for the Association of Stau1 and PNRC2

(A) IP of FLAG-Upf1. HEK293T cells were transiently cotransfected with plasmids expressing FLAG-Upf1, Myc-PNRC2, and Stau1^{55}-HA$_3$, which is the 55 kDa major isoform of human Stau1. Two days after transfection, cells were harvested and lysed. Total-cell RNAs and proteins were purified from the extracts before and after immunoprecipitation (IP) using α-FLAG antibody or mouse (m) IgG as a control.

(B) IPs of PNRC2 variants. HeLa cells were transiently cotransfected with plasmids expressing FLAG-Upf1, Stau1^{55}-HA$_3$, and either Myc-PNRC2 WT, 1–98, or 85–139. IP was performed using α-Myc antibody.

(C and D) IP of Stau1^{55}-HA$_3$ using the extracts of HeLa cells depleted of endogenous Upf1. HeLa cells were transfected with Upf1 siRNA or nonspecific Control siRNA. Two days after transfection, cells were transiently retransfected with plasmids expressing Stau1^{55}-HA$_3$ and Myc-PNRC2. (C) Western blotting of Upf1 to demonstrate the specific downregulation. (D) IP of Stau1^{55}-HA$_3$. IP was performed using α-HA antibody or rat IgG as a control. The levels of coimmunopurified Myc-PNRC2 were normalized to the level of immunopurified Stau1^{55}-HA$_3$. The normalized level in the presence of control siRNA was set to 1.

(E and F) In vivo bimolecular fluorescence complementation (BiFC) analysis for PNRC2-Stau1 association. HeLa cells were transiently transfected with plasmids expressing PNRC2-VN and Stau1-VC with or without FLAG-Upf1. One day later, the cells were fixed and observed under a confocal microscope. Nuclei were stained with DAPI.

Each panel of results is representative of at least two independently performed experiments. See also Figure S2.

bridge PNRC2 and Stau1 in SMD. To test for this, we employed three different approaches: (1) IPs of a PNRC2 variant that lacks the Upf1-binding region, (2) IPs of Stau1 upon downregulation of Upf1, and (3) bimolecular fluorescence complementation (BiFC) technology using yellow venus enhanced fluorescent protein (VFP), which allows for the detection of in vivo protein interactions (Shyu et al., 2006).

For the first approach, we mapped the minimal region of PNRC2 required for binding to Upf1. IP results using PNRC2 variants suggest that the C-terminal region of PNRC2 (amino acids 99 and 130) is essential for binding to Upf1 (Figures S2G–S2I). If Upf1 serves as an adaptor, Stau1 would fail to associate with Myc-PNRC2(1–98), which lacks the Upf1-binding region. As expected, Stau1^{55}-HA$_3$ coimmunopurified with Myc-PNRC2(WT) and 85–139, but not with 1–98 (Figure 2B). Of note, endogenous Dcp1a coimmunopurified with Myc-PNRC2(WT) and Myc-PNRC2(85–139), but not with Myc-PNRC2(1–98), suggesting that the C-terminal region of PNRC2 is essential for associating with Stau1, Upf1, and Dcp1a.

For the second approach, we carried out IPs with extracts of HeLa cells that were depleted of endogenous Upf1 using siRNA and transiently transfected with plasmids expressing Myc-PNRC2 and Stau1^{55}-HA$_3$ (Figures 2C and 2D). Western blotting results revealed that endogenous Upf1 was downregulated to 13% of normal (Figure 2C), and comparable amounts of Myc-PNRC2 and Stau1^{55}-HA$_3$ were expressed before IP (Figure 2D, Before IP). IP results showed that, whereas comparable levels of Stau1^{55}-HA$_3$ were immunopurified, the downregulation of endogenous Upf1 reduced the amount of coimmunopurified Myc-PNRC2 by 3-fold (Figure 2D, After IP).

Third, we employed BiFC technology (Shyu et al., 2006) to test the in vivo interaction between PNRC2 and Stau1 (Figures 2E and 2F). HeLa cells were transiently transfected with (1) plasmid expressing the PNRC2-fused N-terminal half of VFP (VN) and (2) plasmid expressing the Stau1-fused C-terminal half of VFP (VC). Interaction between fused proteins brings the VN and VC fragments within proximity, and they then emit a fluorescence signal (Shyu et al., 2006). The role of Upf1 in the interaction of PNRC2

and Stau1 was tested by overexpressing Upf1 rather than by downregulating endogenous Upf1, because sufficient VFP signals were not observed from cells expressing PNRC2-VN and Stau1-VC (Figure 2E). The transient expression of FLAG-Upf1 significantly increased VFP signals from cells expressing PNRC2-VN and Stau1-VC (Figure 2F). All of these results indicate that Upf1 serves as an adaptor protein for the association of PNRC2 and Stau1.

The Efficiency of SMD Increases and the Efficiency of NMD Decreases during Adipogenesis

Given that (1) PNRC2 is involved in energy homeostasis and obesity, indicative of its possible role in adipogenesis (Zhou et al., 2008), and that (2) PNRC2 functions in both SMD (in this study) and NMD (Cho et al., 2009), it is likely that SMD and/or NMD efficiency may be regulated during adipogenesis. To test for this possibility, we first monitored the protein levels of SMD and NMD factors during adipogenesis in mouse 3T3-L1 cells, which are derivatives of mouse 3T3 cells (Figure 3). Whereas 3T3-L1 cells exhibit a fibroblast-like morphology under normal conditions, these cells differentiate into adipocytes under differentiation conditions.

Oil red O staining (Figure 3A) to detect accumulated lipid droplets and western blotting to detect marker proteins for adipogenesis showed that mouse (m) PPARγ, mCaveolin-1, and mC/EBPβ, all of which serve as marker proteins for adipocytes (Cao et al., 1991; Darlington et al., 1998; Kim et al., 2009a; Lefterova et al., 2008; Yeh et al., 1995), were efficiently induced during adipogenesis (Figure 3B), demonstrating that mouse 3T3-L1 cells were efficiently differentiated into adipocytes under our conditions. Consistent with previous reports (Cao et al., 1991; Darlington et al., 1998; Kim et al., 2009a; Lefterova et al., 2008; Rosen and MacDougald, 2006; Yeh et al., 1995), C/EBPβ was induced early, reaching a maximal level on the second day of adipogenesis. After induction, the level of C/EBPβ decreased sharply before the induction of PPARγ (Figure 3B).

Under the same conditions, we analyzed the levels of SMD and NMD factors. The protein levels of mPNRC2 and mStau1 significantly increased, showing maximal levels on the fourth day of adipogenesis. Intriguingly, whereas the levels of mUpf1 and mUpf2 did not change significantly during adipogenesis, the levels of Upf1 phosphorylation at positions 1,078 and 1,096 increased drastically (Figure 3B). The levels of Stau1, PNRC2, and hyperphosphorylated Upf1 were not significantly changed during the cell cycle (Figure S3), suggesting that the induction of SMD components is specific to adipogenesis itself but not to the cell cycle.

Considering that (1) SMD and a conventional NMD are competitive pathways due to the competition of Stau1 and Upf2 for binding to Upf1 (Gong et al., 2009), and (2) mPNRC2 and mStau1 increase in abundance and mUpf1 becomes hyperphosphorylated during adipogenesis (Figure 3B), increased levels of mPNRC2, mStau1, and hyperphosphorylated mUpf1 may enhance SMD efficiency and, conversely, decrease conventional NMD efficiency during adipogenesis. This possibility was evident from a decrease in the levels of SMD substrates and an increase in the levels of NMD substrates during adipogenesis. qRT-PCRs showed that three cellular SMD substrates, mc-Jun, mSERPINE1, and mPAX3 mRNAs (Gong et al., 2009; Kim et al., 2007), and the exogenous SMD substrate ARF1 mRNA (Kim et al., 2005, 2007) decreased in abundance during adipogenesis (Figures 3C and 3D). On the other hand, exogenously expressed NMD substrates, PTC-containing β-Gl mRNA and PTC-containing GPx1 mRNA (Cho et al., 2009; Kim et al., 2005), increased in abundance during adipogenesis (Figures 3E and 3F). All of these results suggest that the increases in the abundance of PNRC2 and Stau1 and the hyperphosphorylation of Upf1 result in increased SMD efficiency and decreased NMD efficiency during adipogenesis.

SMD Accelerates Adipogenesis

Although the results in Figure 3 suggest that SMD efficiency increases during adipogenesis, it is unclear whether the increase of SMD efficiency is a cause or consequence of adipogenesis. To address this question, mouse 3T3-L1 cells were depleted of NMD or SMD factor using specific siRNA, and then adipogenesis was monitored by western blotting (Figures 4A–4D) and oil red O staining (Figures 4E–4H).

Western blotting showed that downregulation of mStau1, mPNRC2, and mUpf1 delayed the induction of mPPARγ and mCaveolin-1 under differentiation conditions (Figures 4A–4C). Intriguingly, the level of mC/EBPβ was not affected by the downregulations (see the Discussion). All of the western blotting results were quantitated and statistically analyzed (Table S2). As a more quantitative approach, the levels of lipid accumulation in the extracts of oil red O-stained cells were measured by optical density. The results showed that downregulation of mStau1, mPNRC2, or mUpf1 reduced the lipid accumulated during adipogenesis by 2-fold (Figures 4E–4G). Downregulation of mStau1 using another mStau1-1 siRNA that annealed to different sites in mStau1 mRNA showed comparable results (Figure S4). Of note, mUpf2 downregulation did not significantly affect the levels of adipogenic marker proteins (Figure 4D) and lipid accumulation (Figure 4H), suggesting that Upf2-dependent NMD is not relevant to adipogenesis. All these results indicate that increased SMD efficiency accelerates adipogenesis.

Stau1 Interacts with Hyperphosphorylated Upf1 More Strongly during Adipogenesis

Given that hyperphosphorylated Upf1 interacts with PNRC2 more strongly (Cho et al., 2009) and Upf1 functions as an adaptor protein for the interaction between PNRC2 and Stau1 (Figures 2B–2F), hyperphosphorylated Upf1 may interact more strongly with Stau1. The preferential interaction between hyperphosphorylated Upf1 and Stau1 was evident from the following observations.

First, we employed the hyperphosphorylated mutant version of Upf1, Upf1-G495R/G497E (Cho et al., 2009). IP results showed that phosphorylation of FLAG-Upf1-G495R/G497E was increased by ~11-fold compared with FLAG-Upf1-WT (Figure 5A), which is consistent with the previous report (Cho et al., 2009). In addition, Stau1^{55}-HA$_3$ and Myc-PNRC2 coimmunopurified with FLAG-Upf1-G495R/G497E by 18- and 6-fold more, respectively, than with FLAG-Upf1-WT.

Second, treatment with okadaic acid (OA), a potent inhibitor of protein phosphatase 2A that causes accumulation of

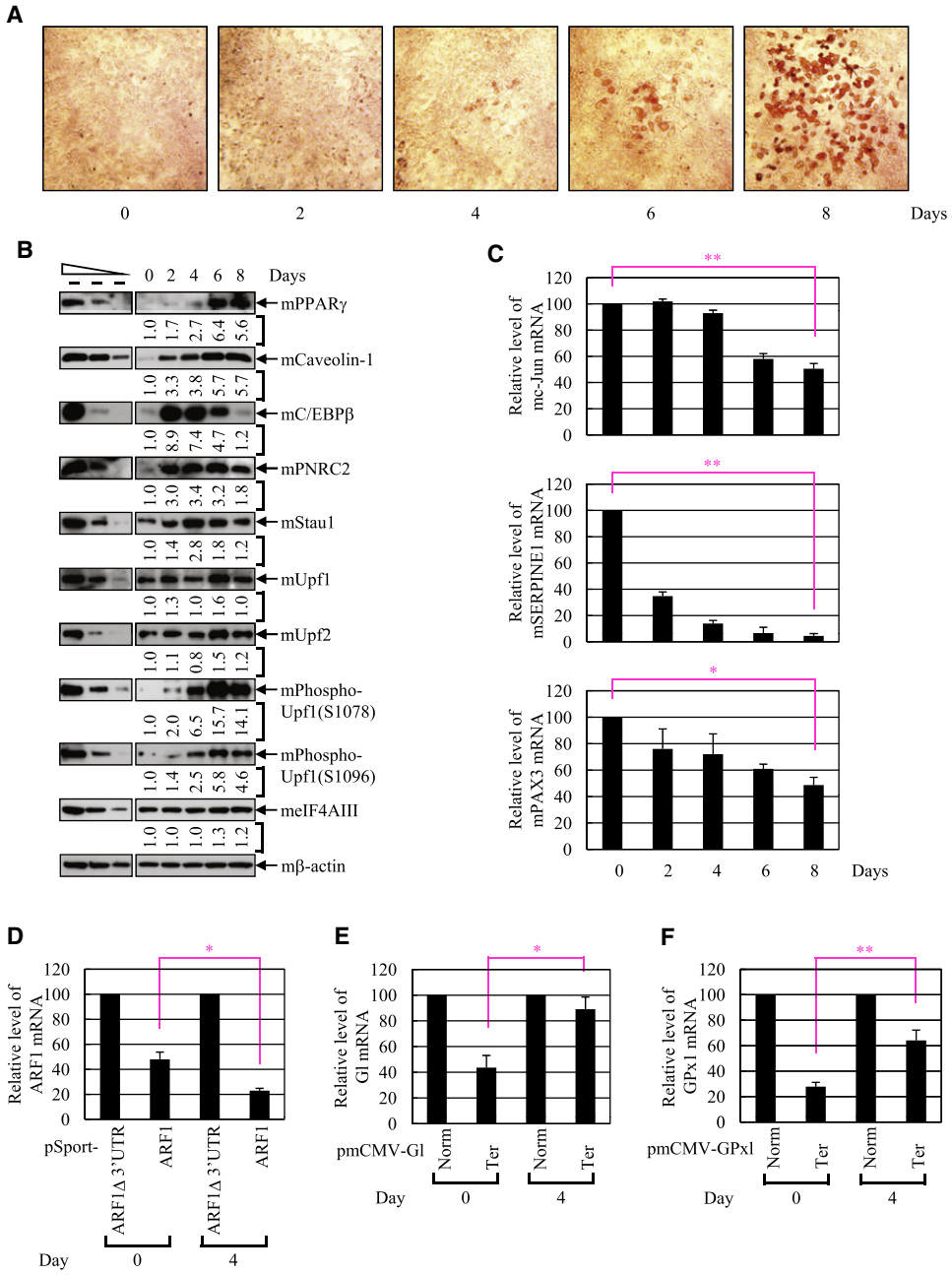

Figure 3. The Efficiency of SMD Increases and the Efficiency of NMD Decreases during Adipogenesis

(A–C) Mouse 3T3-L1 cells were differentiated into adipocytes by treatment with adipogenic cocktail and harvested at the indicated time points. (A) Oil red O staining to demonstrate efficient differentiation under our conditions. The cells were treated with oil red O for 30 min to stain accumulated triglyceride. (B) Western blotting of indicated proteins. The levels of proteins were normalized to the level of mβ-actin. Normalized levels at day 0 of differentiation were set to 1. (C) qRT-PCRs of endogenous mouse (m) SMD substrates, mc-JUN mRNA (top), mSERPINE1 mRNA (middle), and mPAX3 mRNA (bottom) during adipogenesis. The levels of mc-JUN mRNA and mSERPINE1 mRNA were normalized to the level of cellular mSMG7 mRNA. The levels of mPAX3 mRNA were normalized to the levels of mPAX3 pre-mRNA. Normalized levels at day 0 of differentiation were set to 100%.

(D) qRT-PCRs of exogenously expressed SMD substrates. As in (A)–(C), except that pSPORT-ARF1 that did or did not harbor ARF1 3′UTR was transiently transfected 2 days before cell harvest. The levels of ARF1 mRNA were normalized to the level of MUP mRNA. Normalized levels of ARF1 mRNA lacking 3′UTR were set to 100%.

(E and F) qRT-PCRs of exogenously expressed NMD substrates. As in (A)–(C), except that cells were transfected with (1) NMD reporter plasmids pmCMV-Gl and pmCMV-GPx1 that are either PTC-free (Norm) or PTC-containing (Ter) and (2) the phCMV-MUP reference plasmid 2 days before cell harvest. The levels of Gl and GPx1 mRNA were normalized to the level of MUP mRNA. Normalized levels of Gl Norm mRNA and GPx1 Norm mRNA were set to 100%.

The columns and error bars in (C)–(F) represent the mean and standard deviation of at least two independently performed transfections, differentiations, and qRT-PCRs. $^{**}p < 0.01$; $^{*}p < 0.05$. See also Figure S3.

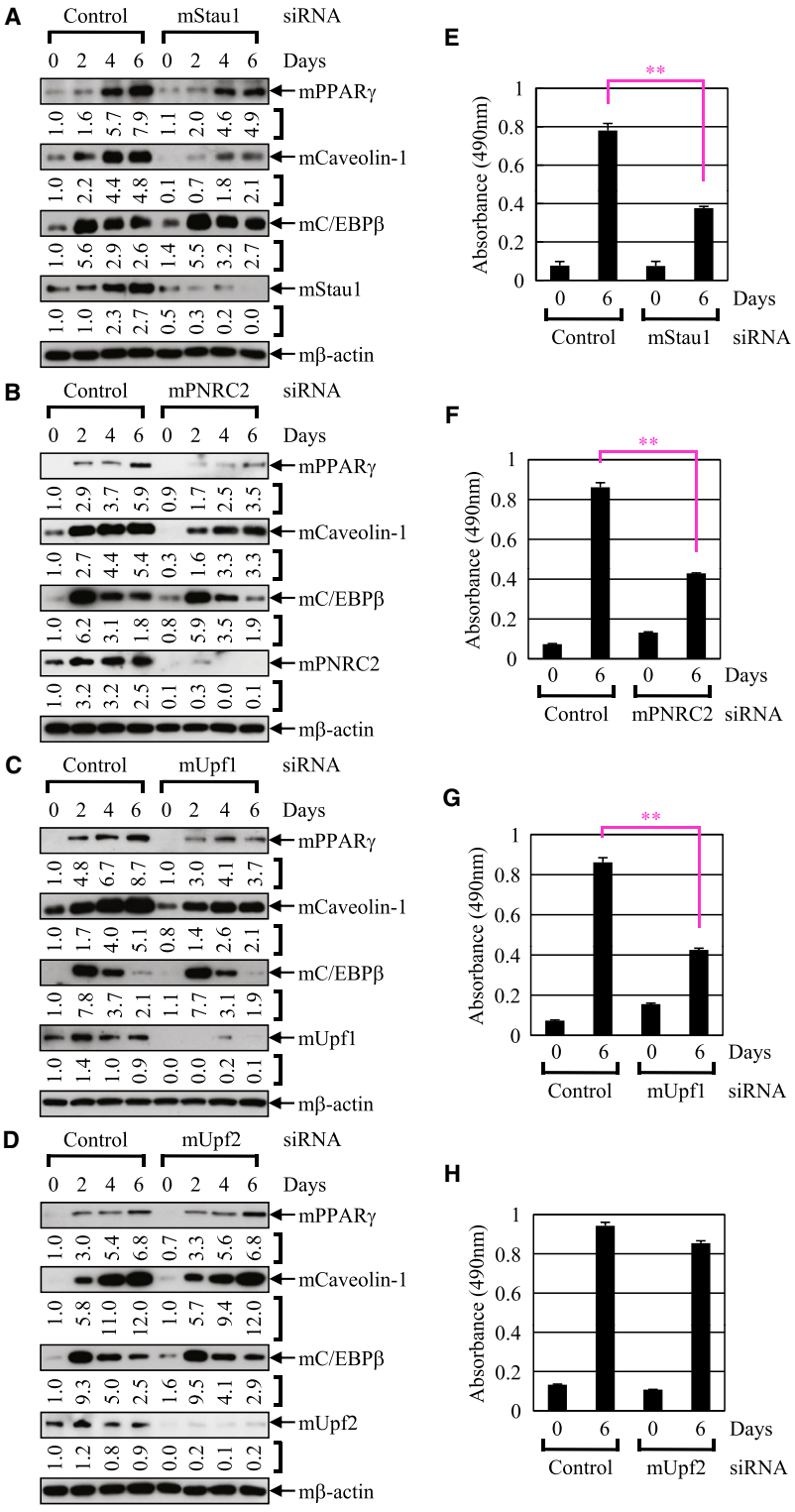

Figure 4. Downregulation of mStau1, mPNRC2, or mUpf1, but Not mUpf2, Leads to Delayed Adipogenesis

Mouse 3T3-L1 cells were transiently transfected with mStau1 siRNA (A), mPNRC2 siRNA (B), mUpf1 siRNA (C), mUpf2 siRNA (D), or nonspecific control siRNA. Cells were then differentiated into adipocytes by treatment with adipogenic cocktail and harvested at the indicated time points.

(A–D) Western blotting of indicated proteins. The levels of proteins were normalized to the level of mβ-actin. Normalized levels in control siRNA-transfected cells at day 0 of differentiation were set to 1.

(E–H) Quantification of accumulated triglyceride. Cells were stained with oil red O for 30 min. The extracts of oil red O-stained cells were prepared, and then the level of staining was quantitated by measuring optical density at 490 nm. The columns and error bars represent the mean and standard deviation of at least two independently performed siRNA transfections, differentiations, and oil red O staining. **$p < 0.01$.

See also Figure S4 and Table S2.

hyperphosphorylated Upf1 within the cells (Cho et al., 2009), increased the level of phosphorylation of FLAG-Upf1-WT by 16-fold and enhanced the interactions of FLAG-Upf1 with Stau1^{55}-HA$_3$ and Myc-PNRC2 by 3-fold and 5-fold, respectively (Figure 5B). All these results indicate that Stau1 interacts with hyperphosphorylated Upf1 more strongly than with hypophosphorylated Upf1.

Considering that Upf1 is hyperphosphorylated during adipogenesis (Figure 3B) and Stau1 interacts more strongly with hyperphosphorylated Upf1 (Figures 5A and 5B), Stau1 might interact with Upf1 more strongly during adipogenesis. This idea was clearly demonstrated by IPs of cellular mUpf1 before and 6 days after differentiation. IP results showed that mUpf1 is 7-fold more hyperphosphorylated after differentiation (Figure 5C), consistent with Figure 3B. Furthermore, mStau1 and mPNRC2 coimmunopurified 10- and 9-fold more strongly with mUpf1, respectively, at 6 days after differentiation than before differentiation (Figure 5C). All these results suggest that the increases in the abundance of PNRC2 and Stau1 and the hyperphosphorylation of Upf1 trigger efficient formation of SMD complex, increase SMD efficiency, and consequently lead to efficient adipogenesis.

Artificial mRNA Harboring 3′UTR of KLF2 mRNA Binds to Stau1, and Its Abundance Is Dependent on Stau1, PNRC2, and Upf1

The observation that SMD accelerates adipogenesis suggests that SMD might target a negative regulator of adipogenesis. Several antiadipogenic proteins have been identified including KLFs, GATA-binding and forkhead families, and CHOP (Rosen and MacDougald, 2006). Intriguingly, KLF2 mRNA was the most upregulated transcript among the transcripts that were commonly regulated upon PNRC2 and Upf1 downregulation (Figure 1A and Table S1). We therefore

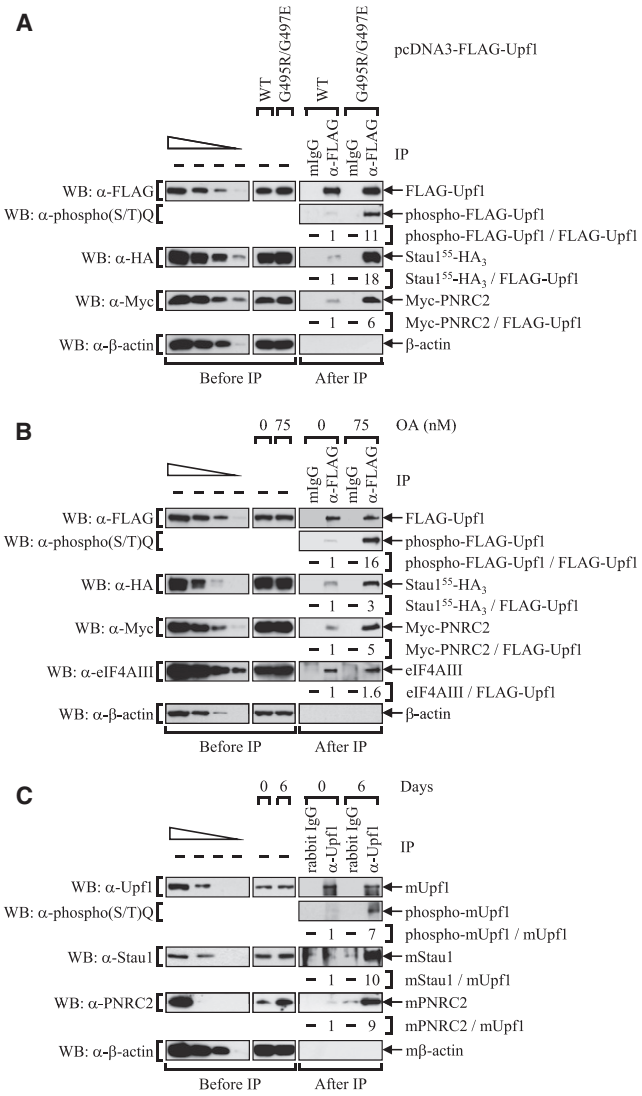

Figure 5. Hyperphosphorylated Upf1 Preferentially Associates with Stau1 and PNRC2

(A) IPs of FLAG-Upf1-WT and FLAG-Upf1-G495R/G497E. As in Figure 2A, except that COS-7 cells were transiently cotransfected with plasmids expressing Stau1^{55}-HA$_3$, Myc-PNRC2, and either FLAG-Upf1-WT and FLAG-Upf1-G495R/G497E. The level of phosphorylation of FLAG-Upf1 was determined by western blotting using α-phospho(S/T)Q antibody. The levels of coimmunopurified proteins were normalized to the level of immunoprecipitated FLAG-Upf1. The normalized level obtained from IP of FLAG-Upf1-WT was set to 1. Cellular β-actin served as a negative control for IP.

(B) IPs of FLAG-Upf1-WT with or without treatment of okadaic acid (OA). HeLa cells were transiently cotransfected with plasmids expressing Stau1^{55}-HA$_3$, Myc-PNRC2, and FLAG-Upf1-WT. Two days after transfection, cells were treated with EtOH (0 nM OA) or 75 nM OA for 5 hr. IP was performed using α-FLAG antibody or mIgG.

(C) IPs of endogenous mUpf1 using extracts of preadipocytes and adipocytes. IPs were performed using α-Upf1 antibody or nonspecific rabbit IgG as a control.

Each panel of results is representative of at least two independently performed experiments.

tested whether KLF2 mRNA is a bona fide SMD target. We first determined whether the 3′UTR of KLF2 mRNA contains a SBS. To this end, we carried out IPs using α-HA antibody to immunopurify Stau1^{55}-HA$_3$ from extracts of cells expressing (1) Stau1^{55}-HA$_3$; (2) MUP mRNA, which lacks a SBS; (3) FLuc-ARF1 SBS mRNA, which contains an Arf1 SBS downstream of the translation termination codon of C-terminally deleted firefly luciferase (FLuc); and (4) FLuc-KLF2 3′UTR mRNA, in which nucleotides 1–467 of the 3′UTR of human KLF2 mRNA were inserted downstream of FLuc (Figure 6A). The α-HA antibody, but not nonspecific rat IgG, immunoprecipitated Stau1^{55}-HA$_3$ (Figure 6B), demonstrating the IP specificity. The RT-PCR results using α-[^{32}P]-dATP and specific oligonucleotides revealed that, whereas no tested mRNAs were detected in IP using rat IgG, FLuc-ARF1 SBS mRNAs and FLuc-KLF2 3′UTR mRNAs, but not MUP mRNAs, were enriched in IP using α-HA antibody (Figure 6C), indicating that the 3′UTR of KLF2 mRNA contains a SBS. Furthermore, downregulation of Stau1, PNRC2, and Upf1, but not Upf2, increased the abundance of FLuc-KLF2 3′UTR mRNAs (Figure 6D), suggesting that KLF2 mRNA is a SMD target.

KLF2 mRNA Is Targeted for SMD during Adipogenesis

To more clearly discern whether KLF2 mRNA is a bona fide SMD target during adipogenesis, we analyzed the relative level and half-life of endogenous mKLF2 mRNAs during adipogenesis. Considering that KLF2 transcriptionally represses PPARγ expression after C/EBPβ induction (Darlington et al., 1998; Rosen and MacDougald, 2006; Rosen and Spiegelman, 2000), the level of mKLF2 mRNAs should be reduced at 2 days after adipogenesis under our conditions (Figure 3B). The qRT-PCR results revealed that, as expected, mKLF2 mRNA was drastically reduced at 2 days after adipogenesis and gradually recovered to the normal level over time in control siRNA-transfected 3T3-L1 cells (Figure 6E). On the other hand, Stau1 downregulation significantly increased the levels of mKLF2 mRNA at all tested time points, showing a 3.5-fold increase in the level of mKLF2 mRNA at 2 days after adipogenesis (Figure 6E). More intriguingly, downregulation of mStau1, mPNRC2, or mUpf1, but not mUpf2, significantly increased the half-life of mKLF2 mRNAs when tested at 2 days after adipogenesis (Figure 6F), indicating that mKLF2 mRNA is a bona fide SMD substrate during adipogenesis.

The Downregulation of KLF2 Rescues the Delay of Adipogenesis Caused by Stau1 or PNRC2 Downregulation

The findings in Figures 3–6 led us to conclude that SMD destabilizes KLF2 mRNA and in turn leads to efficient adipogenesis. If this is the case, downregulation of KLF2 would rescue the delay of adipogenesis caused by Stau1 or PNRC2 downregulation. To test this hypothesis, mouse 3T3-L1 cells were depleted of either Stau1 or PNRC2 with or without downregulation of KLF2. The levels of adipogenesis were then measured by oil red O staining (OD = 490 nm) (Figures 7A and 7B).

Western blotting (Figure 7A) demonstrated specific downregulations by the siRNAs. The oil red O staining showed that downregulation of mStau1 or mPNRC2 reduced the lipid accumulation

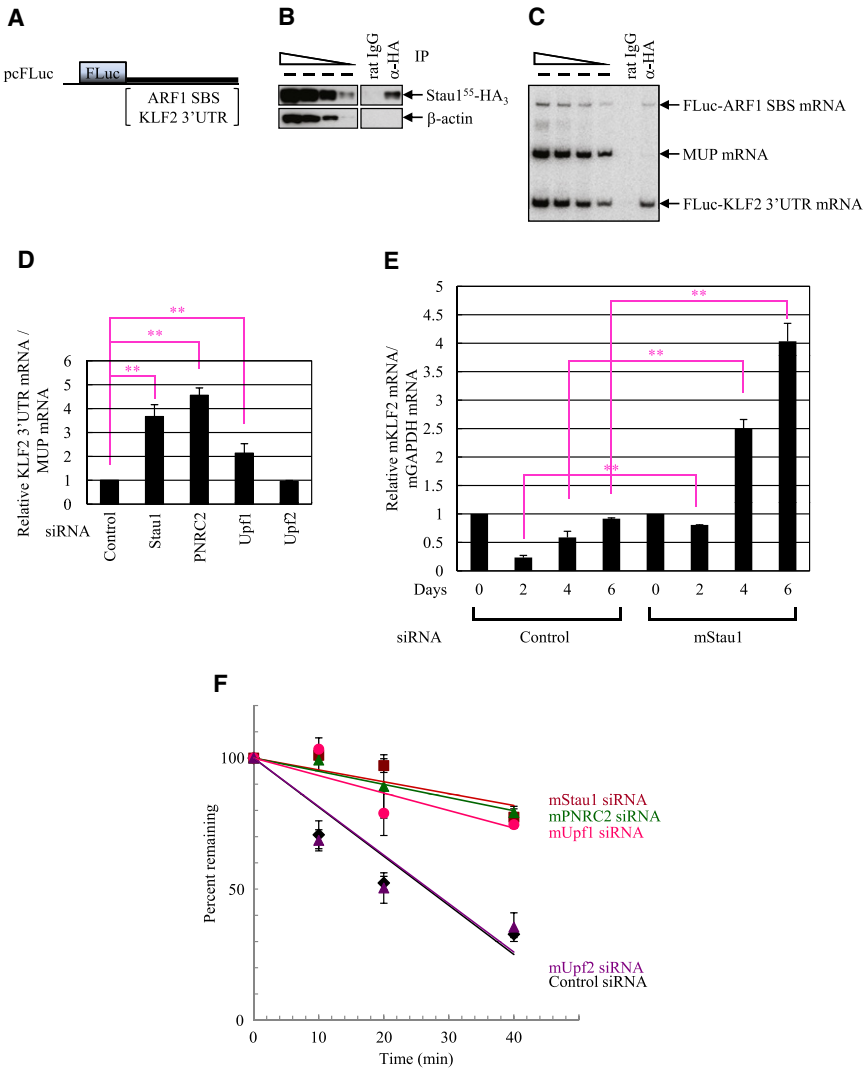

Figure 6. KLF2 mRNA Is a Bona Fide SMD Substrate during Adipogenesis

(A) Schematic diagram of the pcFLuc-ARF1 SBS and pcFLuc-KLF2 3′UTR.

(B and C) IP of Stau1^{55}-HA$_3$. HEK293T cells were transiently cotransfected with (1) Stau1^{55}-HA$_3$ expression plasmid; (2) pcFLuc-KLF2 3′UTR; (3) pcFLuc-ARF1 SBS, which encodes a Stau1-binding site (SBS) of ARF1 3′UTR and serves as a positive control for Stau1^{55}-HA$_3$ binding; and (4) phCMV-MUP, which encodes MUP mRNA that lacks a SBS and serves as a negative control for Stau1^{55}-HA$_3$ binding. IPs were performed using α-HA or nonspecific rat IgG.

(B) The specific IP was demonstrated by western blotting of Stau1^{55}-HA$_3$.

(C) Coimmunopurified mRNAs were analyzed by RT-PCRs using α-[^{32}P]-dATP and specific oligonucleotides.

(D) qRT-PCRs of FLuc-KLF2 3′UTR mRNAs. HeLa cells were transiently transfected with the indicated siRNAs. The level of exogenously expressed FLuc-KLF2 3′UTR mRNA was normalized to the level of MUP mRNA. Normalized level of FLuc-KLF2 3′UTR mRNAs in the presence of control siRNA was set to 1.0.

(E) qRT-PCRs of mKLF2 mRNA during adipogenesis. The level of mKLF2 mRNA was normalized to the level of mGAPDH mRNA. Normalized levels of mKLF2 mRNA in the presence of each siRNA at day 0 were set to 1.0.

(F) Half-life of endogenous mKLF2 mRNA at 2 days after adipogenic induction. Mouse 3T3-L1 cells were transiently transfected with the indicated siRNAs. Cells were treated with 100 μg/ml DRB 2 days after adipogenic induction. Total-cell RNAs were purified at the indicated time points and analyzed by qRT-PCR. The levels of endogenous mKLF2 mRNAs, which were normalized to mGAPDH mRNA, were plotted as a function of time after DRB treatment.

The columns and error bars in (D)–(F) represent the mean and standard deviation of at least two independently performed siRNA transfections, differentiations, and qRT-PCRs. **$p < 0.01$.

during adipogenesis by 2-fold (Figure 7B), consistent with the results in Figure 4. Intriguingly, when both mKLF2 and either mStau1 or mPNRC2 were downregulated at the same time, the levels of accumulated lipid were almost completely restored (Figure 7B), indicating that the downregulation of KLF2 rescues the delay of adipogenesis caused by Stau1 or PNRC2 downregulation. These results also suggest that the delay of adipogenesis caused by downregulation of either Stau1 or PNRC2 is largely due to the increase of KLF2 mRNA.

DISCUSSION

Here we provide molecular insights into the involvement of PNRC2 in SMD. It is quite interesting to compare conventional EJC-dependent NMD and SMD in terms of their molecular mechanisms. In conventional NMD in mammalian cells, Upf1, which is hyperphosphorylated during PTC recognition, is known to interact with several mRNA-degrading enzymes or adaptor proteins: SMG5/7, SMG6, or PNRC2 (Cho et al., 2009; Eberle et al., 2009; Fukuhara et al., 2005; Unterholzner and Izaurralde, 2004; Wilusz, 2009). Depending on which protein interacts with Upf1, NMD substrates would be subject to one or all three decay pathways: 5′-to-3′ decay, 3′-to-5′ decay, and endonucleolytic cleavage (Durand and Lykke-Andersen, 2011; Neu-Yilik and Kulozik, 2008; Nicholson et al., 2010; Rebbapragada and Lykke-Andersen, 2009).

In the case of SMD, Stau1 may functionally replace Upf2 or EJC in NMD. Terminating ribosome may recruit SURF complex during SMD, as in NMD. Consistent with this, Stau1 is complexed with SMG1 (data not shown). After recruitment of SURF complex, Upf1 is hyperphosphorylated by SMG1. Hyperphosphorylated Upf1 then associates with the downstream SBS-bound Stau1 and with PNRC2 more strongly (Figure 5), via the N-terminal one-third (Gong et al., 2009) and the C-terminal two-thirds of Upf1 (Figures S2E and S2F), respectively. In turn, PNRC2 recruits decapping complex via its binding to Dcp1a,

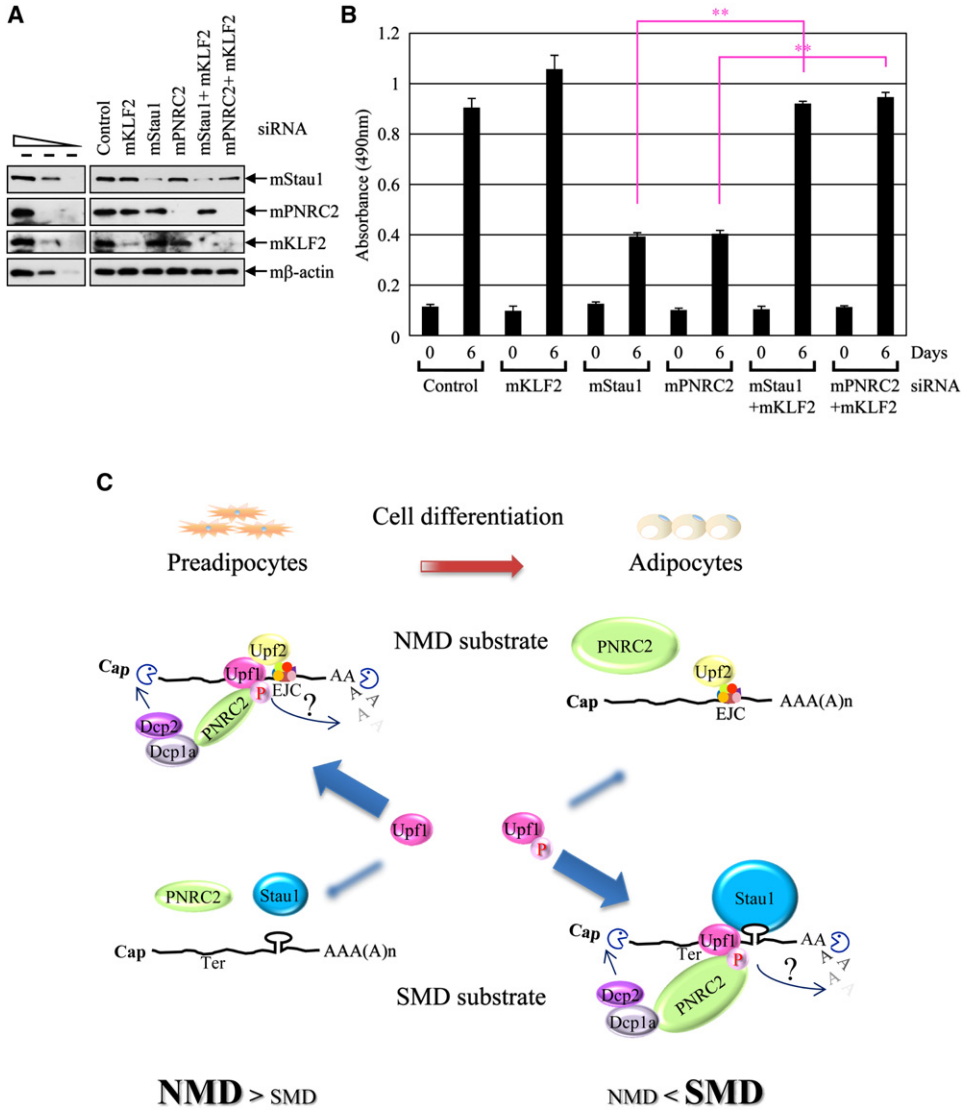

Figure 7. Downregulating KLF2 Alleviates the Delay of Adipogenesis Caused by SMD Inhibition, and a Proposed Model for Competition between SMD and NMD during Adipogenesis

(A and B) Mouse 3T3-L1 cells were transiently transfected with indicated siRNAs. Cells were then differentiated into adipocytes by treatment with adipogenic cocktail. (A) Western blot showing specific downregulation. (B) Quantification of accumulated triglyceride. The columns and error bars represent the mean and standard deviation of two independent siRNA transfections, differentiations, and oil red O staining. **$p < 0.01$.

(C) A model for competition between SMD and NMD during adipogenesis. The sizes of proteins indicate the relative levels of proteins. P specifies a phosphate group in Upf1. The details are provided in the Discussion.

triggering the decapping pathway followed by a rapid 5′-to-3′ decay pathway. Future studies should address whether PNRC2-driven decapping and 5′-to-3′ decay take place following, concurrent with, or independently of 3′-to-5′ decay. In addition, at the step where hyperphosphorylated Upf1 recruits PNRC2 during SMD, hyperphosphorylated Upf1 may recruit other Upf1-binding partners such as SMG5/7 and SMG6, as in NMD, to trigger 5′-to-3′ decay and endonucleolytic cleavage of SMD substrates, respectively. It will also be interesting to determine if SMD and NMD have their own preferences for Upf1-binding partners.

Here we also provide evidence supporting SMD involvement in efficient adipogenesis. Based on these findings, we propose the following model (Figure 7C). During adipogenesis, PNRC2 and Stau1 increase in abundance and Upf1 is hyperphosphorylated (Figure 3B). Stau1 may be induced at the transcriptional level, because Stau1 promoter contains a putative C/EBPβ-binding sequence (data not shown). Hyperphosphorylated Upf1 forms a stable complex with PNRC2 and Stau1 (Figure 5), resulting in increased SMD efficiency (Figures 3C and 3D). SMD then targets and destabilizes KLF2 mRNA (Figure 6), which encodes an antiadipogenic factor (Banerjee et al., 2003; Rosen

and MacDougald, 2006; Wu et al., 2005). The removal of the anti-adipogenic factor by SMD eventually accelerates adipogenesis (Figures 7A and 7B).

In contrast to SMD, conventional (Upf2-dependent) NMD probably does not functionally contribute to adipogenesis. In support of this idea, downregulation of Upf2 had no significant effect on adipogenesis (Figure 4). In addition, considering that SMD and conventional NMD are competitive pathways because Stau1 competes with Upf2 for binding to Upf1 (Gong et al., 2009), the inhibition of Upf2-dependent NMD is likely due to the increase of SMD during adipogenesis (Figure 3). Upf2-independent NMD could also be inhibited as a consequence of Upf1 sequestration by the increased Stau1 during adipogenesis, although we observed that the level of eIF4AIII, which is preferentially involved in Upf2-independent NMD (Gehring et al., 2005), was not changed during adipogenesis (Figure 3).

Adipogenesis involves temporal and sequential induction of transcription factors to regulate a set of gene expression events (Cao et al., 1991; Darlington et al., 1998; Lefterova et al., 2008; Rosen and MacDougald, 2006; Yeh et al., 1995). Early induction of C/EBPβ and C/EBPδ induces C/EBPα and PPARγ, both of which regulate the middle and late stages of adipogenesis (Figures 3 and 4). In particular, induction of C/EBPβ was maximal on the second day of adipogenesis in 3T3-L1 cells, and the level of C/EBPβ decreased sharply before the induction of C/EBPα and PPARγ (Figures 3 and 4). It should be noted that inductions of mPPARγ and mCaveolin-1, but not mC/EBPβ, were affected by the downregulation of mStau1, mPNRC2, or mUpf1 in the present study (Figures 3B and 4A–4D). These results suggest that SMD targets mRNAs expressed after the completion of C/EBPβ induction and before the induction of C/EBPα, PPARγ, and Caveolin-1, all of which are accompanied by the accumulation of cytoplasmic fat (Darlington et al., 1998). Consistent with this idea, we found that KLF2 mRNA, the encoded protein of which transcriptionally targets PPARγ expression after C/EBPβ induction, is a bona fide SMD substrate during adipogenesis (Figure 6). Given that adipogenesis is a highly coordinated process mediated by diverse proteins, however, additional SMD substrates might be involved in the control of adipogenesis. Future studies may reveal a spectrum of mRNAs that not only are targeted for SMD but also play a regulatory role in adipogenesis.

Several previous studies and the present study showed that NMD efficiency decreases during cell differentiation (e.g., muscle and neuron differentiation) in various ways: through (1) the increase of SMD efficiency, (2) an induction of microRNA that silences mRNAs encoding NMD factors, or (3) a direct inhibition of expression of NMD factors (Bruno et al., 2011; Gong et al., 2009). It will be important to determine whether cell differentiation is generally accompanied by a decrease in NMD efficiency and whether the increase of SMD efficiency can generally accelerate cell differentiation.

EXPERIMENTAL PROCEDURES

Plasmid Constructions

The details for plasmid constructions are provided in the Supplemental Experimental Procedures.

Cell Culture and Transfections

COS-7 cells, HeLa cells, HEK293T, and mouse 3T3-L1 cells were used in this study. The details for cell culture and transfections are provided in the Supplemental Experimental Procedures.

Adipogenesis, Oil Red O Staining, and Quantitation of Stained Oil Droplets

Mouse 3T3-L1 cells were cultured in DMEM containing 10% FBS. At 2 days postconfluence, the medium was changed to DMEM containing 10% FBS, 0.25 μM dexamethasone (Sigma), 250 nM insulin (Sigma), and 0.5 mM 3-isobutyl-1-methylxanthine (Sigma) to induce adipogenesis. Two days after induction of adipogenesis, the medium was changed to DMEM containing 10% FBS and 250 nM insulin. Day 0 refers to postconfluent cells immediately before chemical induction of adipogenesis.

To detect accumulated lipid droplets, mouse 3T3-L1 cells were washed twice with PBS and fixed with 10% formalin (Sigma) in PBS for 1 hr at RT. Cells were washed with 60% isopropanol (Sigma), dried, and stained with oil red O solution (Sigma) for 30 min. To remove excess staining, the cells were washed with water and dried. To quantitate the staining, the stained oil droplets in the cell monolayers were dissolved in 100% isopropanol for 10 min. The level of eluted oil red O was then measured at 490 nm.

Quantitative Real-Time RT-PCR and RT-PCR Using α-[^{32}P]-dATP and Specific Oligonucleotides

The details are provided in the Supplemental Experimental Procedures.

Immunoprecipitation and Western Blotting

IPs were carried out as previously described (Cho et al., 2009; Choe et al., 2010; Kim et al., 2009b). Where indicated, phosphatase inhibitors (0.25 mM Na-*o*-vanadate and 10 mM NaF) were included in all buffers during IPs to stabilize the hyperphosphorylated form of Upf1 (Cho et al., 2009). Additional details for IP and western blotting are provided in the Supplemental Experimental Procedures.

Bimolecular Fluorescence Complementation Assay

VFP signals were visualized as described previously (Shyu et al., 2006). Briefly, HeLa cells were transiently cotransfected with the indicated plasmids. One day later, cells were fixed with 2% paraformaldehyde (Merck) and stained with DAPI (Biotium) for nuclei staining. The VFP signals emitted from the cells were then measured with a ZEISS confocal microscope (LSM510 META) using excitation at 500 nm and emission at 535 nm.

Microarray Analysis

Microarray analysis was serviced by Macrogen, Korea. Additional details are provided in the Supplemental Experimental Procedures.

ACCESSION NUMBERS

The microarray data were deposited in the National Center for Biotechnology Information Gene Expression Omnibus web-based data repository under series ID GSE26781.

SUPPLEMENTAL INFORMATION

Supplemental Information includes four figures, two tables, Supplemental Experimental Procedures, and Supplemental References and can be found with this article online at doi:10.1016/j.molcel.2012.03.009.

ACKNOWLEDGMENTS

We thank Lynne E. Maquat for providing NMD reporter plasmids and α-Upf1 antibody, Luc DesGroseillers for plasmid expressing Stau1^{55}-HA$_3$, Jens Lykke-Andersen for plasmid expressing FLAG-Dcp1a, Juan Ortín for anti-human Stau1 antibody, and Young-Gyu Ko and Jeong-Ho Hong for scientific comments. This work was supported by the Korea Healthcare Technology R&D Project (A103001), Ministry for Health, Welfare and Family Affairs, Republic of Korea, and the Korea Science and Engineering Foundation

(KOSEF) Grant funded by the Korea government (MEST) (2009-0078061 and 2009-0084897). H.C., K.M.K., and J.C. were supported in part by a Seoul Science Fellowship. S.H. was supported in part by the project of Global Ph.D. Fellowship, which the National Research Foundation of Korea has conducted since 2011.

Received: May 11, 2011
Revised: October 28, 2011
Accepted: March 5, 2012
Published online: April 12, 2012

REFERENCES

Banerjee, S.S., Feinberg, M.W., Watanabe, M., Gray, S., Haspel, R.L., Denkinger, D.J., Kawahara, R., Hauner, H., and Jain, M.K. (2003). The Kruppel-like factor KLF2 inhibits peroxisome proliferator-activated receptor-gamma expression and adipogenesis. J. Biol. Chem. *278*, 2581–2584.

Bruno, I.G., Karam, R., Huang, L., Bhardwaj, A., Lou, C.H., Shum, E.Y., Song, H.W., Corbett, M.A., Gifford, W.D., Gecz, J., et al. (2011). Identification of a microRNA that activates gene expression by repressing nonsense-mediated RNA decay. Mol. Cell *42*, 500–510.

Cao, Z., Umek, R.M., and McKnight, S.L. (1991). Regulated expression of three C/EBP isoforms during adipose conversion of 3T3-L1 cells. Genes Dev. *5*, 1538–1552.

Cho, H., Kim, K.M., and Kim, Y.K. (2009). Human proline-rich nuclear receptor coregulatory protein 2 mediates an interaction between mRNA surveillance machinery and decapping complex. Mol. Cell *33*, 75–86.

Choe, J., Cho, H., Lee, H.C., and Kim, Y.K. (2010). MicroRNA/Argonaute 2 regulates nonsense-mediated messenger RNA decay. EMBO Rep. *11*, 380–386.

Darlington, G.J., Ross, S.E., and MacDougald, O.A. (1998). The role of C/EBP genes in adipocyte differentiation. J. Biol. Chem. *273*, 30057–30060.

Durand, S., and Lykke-Andersen, J. (2011). SnapShot: nonsense-mediated mRNA decay. Cell *145*, 324–324.

Eberle, A.B., Lykke-Andersen, S., Muhlemann, O., and Jensen, T.H. (2009). SMG6 promotes endonucleolytic cleavage of nonsense mRNA in human cells. Nat. Struct. Mol. Biol. *16*, 49–55.

Eulalio, A., Behm-Ansmant, I., and Izaurralde, E. (2007). P bodies: at the crossroads of post-transcriptional pathways. Nat. Rev. Mol. Cell Biol. *8*, 9–22.

Fukuhara, N., Ebert, J., Unterholzner, L., Lindner, D., Izaurralde, E., and Conti, E. (2005). SMG7 is a 14-3-3-like adaptor in the nonsense-mediated mRNA decay pathway. Mol. Cell *17*, 537–547.

Gehring, N.H., Kunz, J.B., Neu-Yilik, G., Breit, S., Viegas, M.H., Hentze, M.W., and Kulozik, A.E. (2005). Exon-junction complex components specify distinct routes of nonsense-mediated mRNA decay with differential cofactor requirements. Mol. Cell *20*, 65–75.

Gong, C., and Maquat, L.E. (2011). lncRNAs transactivate STAU1-mediated mRNA decay by duplexing with 3′ UTRs via Alu elements. Nature *470*, 284–288.

Gong, C., Kim, Y.K., Woeller, C.F., Tang, Y., and Maquat, L.E. (2009). SMD and NMD are competitive pathways that contribute to myogenesis: effects on PAX3 and myogenin mRNAs. Genes Dev. *23*, 54–66.

Huntzinger, E., Kashima, I., Fauser, M., Sauliere, J., and Izaurralde, E. (2008). SMG6 is the catalytic endonuclease that cleaves mRNAs containing nonsense codons in metazoan. RNA *14*, 2609–2617.

Kashima, I., Yamashita, A., Izumi, N., Kataoka, N., Morishita, R., Hoshino, S., Ohno, M., Dreyfuss, G., and Ohno, S. (2006). Binding of a novel SMG-1-Upf1-eRF1-eRF3 complex (SURF) to the exon junction complex triggers Upf1 phosphorylation and nonsense-mediated mRNA decay. Genes Dev. *20*, 355–367.

Kim, Y.K., Furic, L., Desgroseillers, L., and Maquat, L.E. (2005). Mammalian Staufen1 recruits Upf1 to specific mRNA 3′UTRs so as to elicit mRNA decay. Cell *120*, 195–208.

Kim, Y.K., Furic, L., Parisien, M., Major, F., DesGroseillers, L., and Maquat, L.E. (2007). Staufen1 regulates diverse classes of mammalian transcripts. EMBO J. *26*, 2670–2681.

Kim, K.B., Kim, B.W., Choo, H.J., Kwon, Y.C., Ahn, B.Y., Choi, J.S., Lee, J.S., and Ko, Y.G. (2009a). Proteome analysis of adipocyte lipid rafts reveals that gC1qR plays essential roles in adipogenesis and insulin signal transduction. Proteomics *9*, 2373–2382.

Kim, K.M., Cho, H., Choi, K., Kim, J., Kim, B.W., Ko, Y.G., Jang, S.K., and Kim, Y.K. (2009b). A new MIF4G domain-containing protein, CTIF, directs nuclear cap-binding protein CBP80/20-dependent translation. Genes Dev. *23*, 2033–2045.

Lefterova, M.I., Zhang, Y., Steger, D.J., Schupp, M., Schug, J., Cristancho, A., Feng, D., Zhuo, D., Stoeckert, C.J., Jr., Liu, X.S., et al. (2008). PPARgamma and C/EBP factors orchestrate adipocyte biology via adjacent binding on a genome-wide scale. Genes Dev. *22*, 2941–2952.

Maquat, L.E., and Gong, C. (2009). Gene expression networks: competing mRNA decay pathways in mammalian cells. Biochem. Soc. Trans. *37*, 1287–1292.

Mendell, J.T., Sharifi, N.A., Meyers, J.L., Martinez-Murillo, F., and Dietz, H.C. (2004). Nonsense surveillance regulates expression of diverse classes of mammalian transcripts and mutes genomic noise. Nat. Genet. *36*, 1073–1078.

Miki, T., Takano, K., and Yoneda, Y. (2005). The role of mammalian Staufen on mRNA traffic: a view from its nucleocytoplasmic shuttling function. Cell Struct. Funct. *30*, 51–56.

Neu-Yilik, G., and Kulozik, A.E. (2008). NMD: multitasking between mRNA surveillance and modulation of gene expression. Adv. Genet. *62*, 185–243.

Nicholson, P., Yepiskoposyan, H., Metze, S., Zamudio Orozco, R., Kleinschmidt, N., and Muhlemann, O. (2010). Nonsense-mediated mRNA decay in human cells: mechanistic insights, functions beyond quality control and the double-life of NMD factors. Cell. Mol. Life Sci. *67*, 677–700.

Parker, R., and Sheth, U. (2007). P bodies and the control of mRNA translation and degradation. Mol. Cell *25*, 635–646.

Rebbapragada, I., and Lykke-Andersen, J. (2009). Execution of nonsense-mediated mRNA decay: what defines a substrate? Curr. Opin. Cell Biol. *21*, 394–402.

Roegiers, F., and Jan, Y.N. (2000). Staufen: a common component of mRNA transport in oocytes and neurons? Trends Cell Biol. *10*, 220–224.

Rosen, E.D., and MacDougald, O.A. (2006). Adipocyte differentiation from the inside out. Nat. Rev. Mol. Cell Biol. *7*, 885–896.

Rosen, E.D., and Spiegelman, B.M. (2000). Molecular regulation of adipogenesis. Annu. Rev. Cell Dev. Biol. *16*, 145–171.

Shyu, Y.J., Liu, H., Deng, X., and Hu, C.D. (2006). Identification of new fluorescent protein fragments for bimolecular fluorescence complementation analysis under physiological conditions. Biotechniques *40*, 61–66.

Unterholzner, L., and Izaurralde, E. (2004). SMG7 acts as a molecular link between mRNA surveillance and mRNA decay. Mol. Cell *16*, 587–596.

Wilusz, J. (2009). RNA stability: is it the endo' the world as we know it? Nat. Struct. Mol. Biol. *16*, 9–10.

Wu, J., Srinivasan, S.V., Neumann, J.C., and Lingrel, J.B. (2005). The KLF2 transcription factor does not affect the formation of preadipocytes but inhibits their differentiation into adipocytes. Biochemistry *44*, 11098–11105.

Yamashita, A., Kashima, I., and Ohno, S. (2005). The role of SMG-1 in nonsense-mediated mRNA decay. Biochim. Biophys. Acta *1754*, 305–315.

Yamashita, A., Izumi, N., Kashima, I., Ohnishi, T., Saari, B., Katsuhata, Y., Muramatsu, R., Morita, T., Iwamatsu, A., Hachiya, T., et al. (2009). SMG-8 and SMG-9, two novel subunits of the SMG-1 complex, regulate remodeling of the mRNA surveillance complex during nonsense-mediated mRNA decay. Genes Dev. *23*, 1091–1105.

Yeh, W.C., Cao, Z., Classon, M., and McKnight, S.L. (1995). Cascade regulation of terminal adipocyte differentiation by three members of the C/EBP family of leucine zipper proteins. Genes Dev. *9*, 168–181.

Zhou, D., Shen, R., Ye, J.J., Li, Y., Tsark, W., Isbell, D., Tso, P., and Chen, S. (2008). Nuclear receptor coactivator PNRC2 regulates energy expenditure and adiposity. J. Biol. Chem. *283*, 541–553.